A Comparative Analysis On Finding Out Electrolytes From Effective Data Sets In Human Sweat.

By

MD. SHAHRIAR SADID (160021035)

SAYEF SHAHRIAR (160021147)

ABBA MAHAMAT (170021167)

A Thesis Submitted to the Academic Faculty in Partial Fulfillment of the

Requirements for the Degree of

Bachelor of Science in Electrical and Electronic Engineering

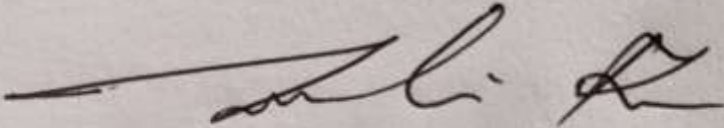Department of Electrical and Electronic Engineering

Islamic University of Technology (IUT)

Gazipur, Bangladesh

May,2022

A Comparative Analysis On Finding Out Electrolytes From Effective Data Sets In Human Sweat.

Approved by

Dr. Md. Taslim Reza

Supervisor and Professor
Department of Electrical and Electronic Engineering (EEE)
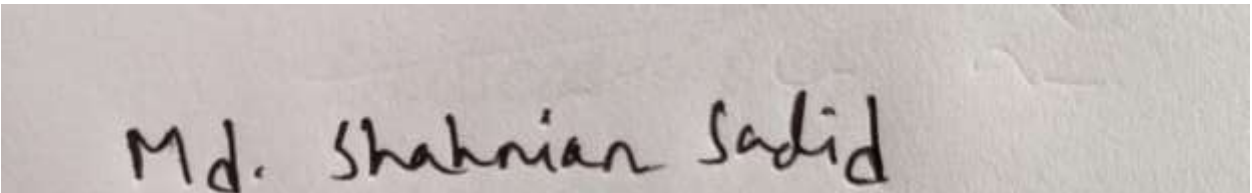Islamic University of Technology (IUT)
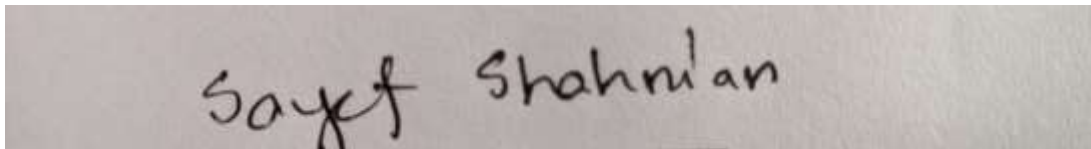Gazipur-1704, Bangladesh
Date:

Declaration of Authorship

This is to certify that the work presented in this thesis paper is the outcome of research carried out by the candidates under the supervision of Dr. Md. Taslim Reza, Professor, Department of Electrical and Electronic Engineering (EEE), Islamic University of Technology (IUT). It is also declared that neither this thesis paper nor any part thereof has been submitted anywhere else for the reward of any degree or any judgement.
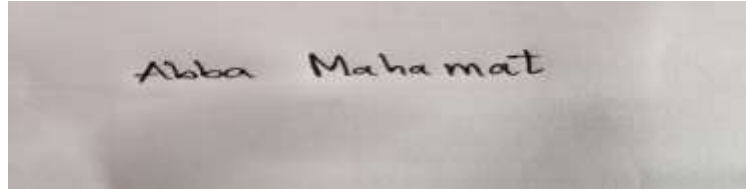
Authors

Md. Shahriar Sadid

_____

Md. Shahriar Sadid
ID-160021035

Sayef Shahrian

_____

Md. Sayef Shahriar
ID-160021147

Abba Mahamat
ID-170021167

Dedicated to
The Almighty, without whom nothing is ever possible.

TABLE OF CONTENTS

Chapter 1

Introduction

Chapter 2

Literature Review

Chapter 3

Methodology

Chapter 4

Results and Discussion

Chapter 5

Conclusion

List Of Figures

<u>ACKNOWLEDGEMENTS</u>

Abstract

This paper explores the non-invasive method of identifying electrolyte levels of human sweat. A non- invasive micro patch antenna-based sensor is used to determine the electrolyte level of human sweat. This device is designed to be wearable so as to have close proximity to the human skin in order to have great advantage in detecting the electrolyte (NaCl) level from sweat. A 1.8 mm thick copper patch antenna that operate in a frequency range of 0.5 GHz -3.5 GHz is used. Paper based substrate is preferred due to the fact that it's a good absorber and cost effective. For testing the sensitivity, the antenna is structured to have a frequency of 1.57 GHz with several dielectric constants ranging between 1.0 F/m - 2.0 F/m, thereby allowing the substrate dielectric to be controlled by the properties of the absorbed sweat. The paper looks at the Shift in resonant frequency and also the magnitude of reflection coefficient which is employed on a concentration range of approximately 0.001 mol/L - 5 mol/L of NaCl. For various levels of electrolyte, the resonant frequency, the reflection magnitude are fluctuating, the first resonance is regarded for analysis of data.

Chapter 1

Introduction

1.1 Introduction

The aging population and rapidly rising health-care expenses have sparked a surge in interest in wearable medical sensors (WMSs). In the past, raw medical data was sensed and stored by in-hospital monitoring devices such as electrocardiogram (ECG) and electroencephalogram (EEG) monitors, with processing done later on another system, such as an external computer [1]. Several advances in communication, signal processing, machine learning, and biological sensing have come together to bring continuous health monitoring closer to reality. The development of Internet-connected WMSs which can non-invasively sense, collect, and even process many forms of body-related data, like as electrical, thermal, and optical signals created by the human body is at the forefront of these trends.

1.2 Significance of the research

Despite the emergence of numerous WMS-based systems in recent years, potential challenges associated with their design, development, and implementation have not been well addressed. The main objective of this research is to give researchers new to the field an opportunity to explore the applications offered by such systems, their constituent components, challenges associated with their design and development, and how previous research studies have attempted to address these challenges. Every average adult human secretes between 600 ml and 700 ml of hypnotic fluid which is secreted by the sweat gland per day. Sweat can easily be retrieved from the surface of the skin of the body, this sweat is secreted by special gland (nectarine gland) and they contain electrolytes like (NaCl), because of this easy access of the sweat on the body, accessing it through noninvasive method gives it more advantage over other body fluids like blood.

Rich physiological biomarker is abundant in human sweat which makes it preferable for noninvasive hydration monitoring. Among the fluids used are electrolytes, proteins and amino acid. Biomarkers in sweat composition are used to detect genetic conditions, elevated chloride levels used to test cystic fibrosis or its related diseases especially those caused by sodium loss and also for observing glucose level, a measure of the correlation between sweat and blood level has been effective in use lately. Information for skin is also made available through the measure of the temperature of the skin surface.

Human dehydration by microwave signals is reported in several studies lately. Losses and absorption of electromagnetic waves vary from fluid to fluid in the body due to their different electrolytic concentration which signals are broadcast or communicated that has encouraged the development of microwave-based sensor for noninvasive body fluid monitoring. Reflection or transmission analysis are mostly used for the assessment of water content in the body.

The substrate inscribes between the top and bottom, the radiating microstrip patch element and the feed line of the microstrip is fed to the substrate in a basic slot linked patch antenna. These two substrates thickness and dielectric constants have to be selected individually in order to maximize the unique electrical circuitry function and radiation. The first original antenna sample had a circle like integrated slot which has bought to knowledge that by using an etched that is rectangular, can enhance the quality of the integration of a particular space on area which result from the divergence

of improve magnetic field over a dozen of material and dimension factors are involved in the departure coupled microstrip antenna thus an outline on the course of change on the following variables. The dielectric constant of the antenna substrate the width of the device the dielectric constant of the field substrate, length of slot, line, the position of the feed line with respect to the slot of the device and the position of the patch with respect to slot to separate the patch and microstrip feed line, a ground plane is used in order to reduce spurious radiation there is a coupling that exist on the patch antenna together with the feed line (often centered under patch).

There have been numerous health methods that have summoned several outstanding recognition by health personnel's among which is the non-invasive electrolyte monitoring approach which has recently been brought as a health indication. This device will help replace the cumbersome laboratory equipment in use to a lighter and simpler systems. The device will be of handy for patient with heart diseases, dialysis problem, kidney disease etc. This can greatly influence and improve on the cost recovery by cutting down cost of health care problems. Exercises can also contribute immensely in dehydration and imbalance in electrolyte of the body system which is needed by non-invasive system. There are several dehydration assets that require regular electrolyte level check- up which is made simple by non-invasive process that uses only one sensor instead of several amount of sample which is not only costly but also time consuming. In a nutshell the non-invasive method due to its durability and flexibility which uses sensor, do not require regular changes.

Laboratories are now using an outstanding analytical method called potentiometer based on ion selective electrode whose popular usage is rooted in its modern lordly analytic characteristics which enables a high and flexible observation of ions on the worktop in a wider area feedback (a magnitude of 3 to 5), with a continuous time of response which is remarkably low in cost and also with a signal of near zero current which enables end users to have an easy analysis of ion content sample.

Patch antennas are very light, comparatively small in size with a low profile, cost effective, wide band frequency, great efficiency, grater adaptability to the environment, low risk of radiation to the body, etc.

Varieties of antenna have been discovered to date, and they are employed in a variety of medical and pharmaceutical applications. Radiation of Electromagnetics with frequencies range from 300 MHz to 300 GHz is used to broadcast these waves, which makes them the most commonly used embedded antenna. They are characteristically simple to manufacture which is also very important in transceiver system. Though with a low band width, it has been in use of recent years in modern communication.

Verily, due to the advance in technology to 5G, the incorporation of patch antenna has become all important.

This work is basically exploring how microwave signals identify the condition of hydration from sweat of the body. The device works on an average range of 0.5 GHz -3.5 GHz and encapsulates a patch antenna planted on a paper substrate. With an average height of 30 mm, the device (sensor) is designed to operate directly on the skin.

One of the main objectives of the analysis made in this write up is based on the simplicity of wearable electrolyte monitoring by looking at the manner at which an efficient micro strip patched antenna is designed, considering the electromagnetic waves, frequency domain interface, line patch antenna via COMSOL Multi-physics\ 5.4a software. The antenna is modeled to have multiple of substrates which are taken in by line-feeding method. In order to measure its sensitivity, we take into consideration the changes in the level of magnitude of reflection coefficient and also having in mind the frequency(resonant) of the device.

Wearable medical sensors (WMSs) are receiving increasing interest from the scientific community and the business sector. WMS-based systems have begun to revolutionize our daily life, as a result of technical improvements in sensing, wireless connection, and machine learning. Despite the fact that WMSs were initially designed to facilitate low-cost solutions for continuous health monitoring, the applications of WMS-based solutions today extend much beyond the medical field. Several studies have recommended the usage of education, human-computer interaction, and security are examples of varied application sectors where such systems are utilized.

In spite of the fact that the number of such research studies has increased dramatically in recent years, the possible obstacles connected with their design, development, and implementation are neither well-studied nor widely acknowledged [10].

In the past five years, digital wellness wearables that can gather data in real time and expose the physical and chemical features of the body to evaluate wellness have increased. Wearables are small electronic devices that, when worn on the body, may measure temperature, blood pressure, blood oxygen, breathing rate, sound, GPS position, elevation, physical movement, and changes in direction, as well as the electrical activity of the heart, muscles, brain, and skin.

This wealth of information may be used to monitor calorie expenditure, exercise, stress, good posture, poor sleep quality, cognitive decline, and even early warning indications of infection or inflammation. What we cannot measure, we cannot manage. Wearables can enable us to continuously monitor our health and well-being without needing to attend a clinical center and to take fast action if necessary.

Wearables could potentially alert us to modifiable risk factors that could negatively impact our health and well-being. In a recent study [12], for instance, employees aware employed with wearables to measure the stress and sleep quality of office workers and it was discovered that extended exposure to dry, indoor air may increase their stress level during work hours, leading to poor sleep quality and lower physical fitness.

1.3 Objective Of The Research

The main reasons behind conducting this study are as follows:

**To make it easy for all people who may or may not be afraid of needles to go to the clinic and have health checkup.

**To make wearable devices easily accessible for people all across the globe.

**To find the minimum error possible in these devices.

✳✳To find the health chart analysis in a week and at the end of the year make a big data analysis to give people easy access about their health chart.

✳✳Make easily accessible good product life with as low cost as possible.

1.4 Major contributions

This thesis makes the following major contributions based on the above-mentioned research objectives:

✳✳ Two different methods are proposed naming as S11 calculation and FFT calculation which are analyzed from the data taken after the simulation at different concentration from different software modules.

✳✳For 2nd method, Five different areas of interest are proposed for which the error was calculated in order to incorporate with the original one.

✳✳ For the 1st method the interest is basically for the resonant frequency to the concentration which was further analyzed to find out the error at different modes of operation.

1.5 Thesis outline

Subjected to the things mentioned above, the thesis is outlined as follows:

It is anticipated that Chapter 1 will offer the context and rationale for this investigation, including the significance of this research, its major contributions, and its intended outcomes. The thesis outline is also supplied at the conclusion of this chapter.

Chapter 2 focuses on a survey of quantitative analysis and procedures-related literature, as well as the theoretical and research elements of significant contemporary studies.

Chapter 3 covers the methodology presented for this research, a comprehensive examination of the procedures and strategies performed in an effort to extract the parameters used to distinguish between the two proposed methods. It also analyzes the effect of the numerous variables on the study's outcome.

Chapter 4 discusses all the results obtained and give a clear explanation about what each figure signifies and at the end it also includes several tables to indicate the error.

The fifth chapter summarizes and closes the work by discussing future research directions in this field.

Chapter 2

Literature Review

2.1 Literature Review and Previous Works

WMSs enable proactive prevention and remote detection of health issues, thus with the potential to significantly reduce health care costs [2], [3]. Since the introduction of the first wearable heart monitor in 1981 [4], numerous types of WMS-based systems have been proposed, ranging from simple accelerometer-based activity monitors [3], [4] to complex sweat sensors [5]. WMS-based systems have also been developed for continuous long-term health monitoring [1], [6]. In the last decade, with the pervasive use of Internet connected WMSs, the scope of applications of WMS based systems has extended far beyond health care. For example, such systems have targeted application domains as diverse as education, information security, and human-computer interaction (HCI). Park et al. [7] introduced a WMS-based teaching assistant system, called SmartKG. It collects, manages, and fuses data gathered by several wearable badges to prepare valuable feedback to the teacher. Mosenia et al. [8] proposed a continuous authentication system based on WMSs, called CABA. They demonstrated how an ensemble of medical data streams, i.e., a sequence of biomedical signal samples, enables accurate continuous user authentication. Barreto et al. [9] designed and implemented an EEG/Electromyogram (EMG) human-computer interface,

which uses biomedical signals gathered from the subject 'shed to control computer cursor movements.
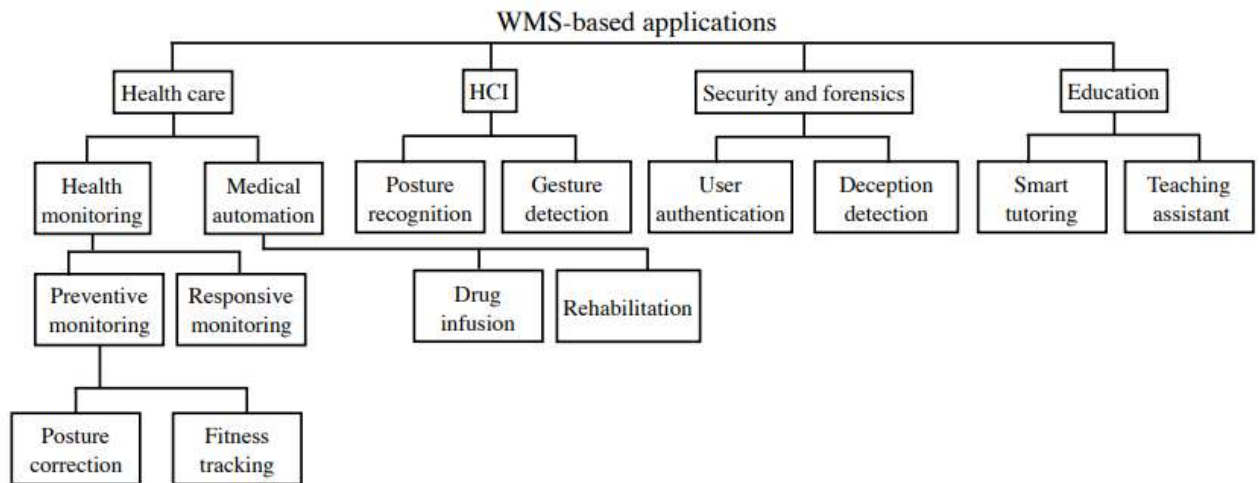

Figure 1.1: Scopes of different WSM based applications [10].

In the case of continuous monitoring, a portable sensor for non-invasive electrolyte monitoring is particularly beneficial. Although research on noninvasive blood glucose monitoring has emerged, it does not provide accurate results [14]. Some currently available wearable sensors for sweat monitoring are prohibitively expensive for mass distribution, and their design process is so intricate that it requires highly skilled personnel to deploy in practice [15]. Sodium and chloride levels in sweat are indicators used to determine an athlete's hydration condition, but excessive ammonium levels are associated with acute weariness [16]. Brendtke et al. employed the frequency range of 7.0 GHz to 9.50 GHz to assess hydration status by analyzing water content in skin tissue [17].

In the health care system non-invasive electrolyte supervision sensor is a very useful instrument for a constant record tracking. The other non-invasive techniques like blood glucose check seems not to provide reliable results. Potentiometer sensor due to their flexible nature here attracted several interests based on the fact that they are greatly used in clinical and other applications,

mostly on that related to body sweet. The Na and Cl in body fluid (sweat) are commonly used in checking the hydration nature in gymnasts and sports for both men and women. As mentioned earlier, most sensors are difficult to design and very costly, hence making it practically difficult to execute especially in large quantity, an advance in the area of microwave technology is being developed for checking the permittivity of matter which has widely been in use for the design of the antenna, circuit (microwave) etc. All these sensors are biomedical in nature. A 7 GHz to 9.5 GHz range of frequency was designed to observe the nature of liquid on the surface of the skin. The overall aim was centered around building a parallel contrived skin that houses a certain value of NaCl content that is put through to adapt to the changes on the skin and keeps track on sensitivity of the frequency.

A low-cost copper patched antenna made of paper substrate that's 95-97 mm is used in this work, paper substrate is chosen over plastic for the design of the antenna because the plastic matter is neither biodegradable nor cost effective as compared to the paper method. Mostly due to the absorption nature of paper over plastic, we've chosen to use the paper. The design is a three layers type with Ws = 135 mm and Ls = 135 mm in thickness. The upper, middle and lower layers are the patch, dielectric and the ground plane as the terminal in the electromagnetic frequency domain. Impedance 50 ohms and 2 volt is used through excitation of the lumped port to construct the port. The inside of the device has width which is denoted by WL = 5.6 mm and length denoted in the paper by Lsb = 19 mm respectively. For the other part of the design a high level of NaCl, which according to Peymen et al. [13] has a connection with the conductivity of the substance, concentration of the substance by the use of Cole-Cole model of NaCl [13] attributes at frequency of microwave level. Recent techniques for non-invasive body electrolyte monitoring from electrocardiography cannot be effectively applied to these three age groups due to their complexity, and electrocardiograph test results do not reveal the majority of changes in body electrolytes, but rather mainly potassium [18]. Emerging research on blood glucose monitoring utilizing noninvasive methods does not provide accurate results [19].

On the third phase of the design value of 1 F/m, 1.5 F/m and 2 F/m dielectric constants are used for various sensors values for paper substrate having permittivity of different relativity in between the ground plane and copper patch houses the substrate matter. An occurrence of 1.57 GHz

resonance of $\varepsilon r = 1$ F/m having a coefficient of reflection of about -22.5 dB is utilized for different sensor having a similar dielectric constant, the NaCl concentration is about 0.03 mol/L, 0.05 mol/L, 0.07 mol/L and 0.02 mol/L there will be a change in the resonance frequency from 1.574 GHz to 1.6 GHz and 0.05 mol/L, 0.09 mol/L, 0.1 mol/L concentration for the other values of frequency 1.682 GHz, 1.7 GHz and 1.75 GHz

Various sensors and chips have been miniaturized, this has resulted from tremendous advancements in the domains of micro-electronics circuits and integrated domain. Medical implants, hypothermia therapies, and monitoring wireless wellness are just a few of the medical applications where antennas have been employed for a long time. An antenna is a device that can received or transmit Electromagnetic radiation in general. The equipment that converts radio frequency signals into electromagnetic wave signals are known as antennas. Various varieties of antenna have been discovered to date, and they are employed in a variety of medical and pharmaceutical applications. Electromagnetic wave with frequencies ranging from 300 MHz to 300 GHz is used to broadcast these waves. Recent advancements in microwave technology are being implemented for measuring the permittivity of materials and are seen as crucial for antenna design [20].

These antennas include reflector antennas, aperture and lens antennas, patch antennas, and printed patch antennas. The fabrications on these printed microstrip patch antennas are made using photo lithography technology. The microstrip patch antenna is the most simple and advanced sort of printed antenna. The patch antenna (MSPA) is the most widely used microstrip patch antenna for health care applications due to its advantages over other types of antennas.

The radiative micro-strip patch element is engraved on the surface of the antenna structure, as well as the microstrip feed line is carved just on bottom of the feeding material in a basic angle linked patch antenna. Therefore, the dielectric properties and density of these two components can be chosen independently to enhance the various electric operations of photons and circuitry. Notwithstanding the fact that the original sample antenna had a round coupling aperture, it was immediately learned that by using a triangular slot would enhance coupling for just a certain projection angle for its enhanced magnetic charge density.

Outlining the basic patterns with modification of these parameters for the aperture paired microstrip antenna, that includes more than twelve component and physical characteristics: intake substrate feed substrate depth, slot thickness, dielectric constant, slot size, feed path length, feed line position in relation to vacant spot, stance of the patch comparative to groove, micro-strip patch width, constant, antenna substrate thickness, antenna substrate dielectric ,micro-strip patch length, feed substrate dielectric constant, feed substrate thickness, slot length, slot width, feed line width, feed line position relative to slot, transmission position in relation to slot.

2.2 Design Solution

The antenna has been designed from another paper taken as reference [12] from where the design is basically selected and the value of the different parameters has been tweaked a little in order to make sure that the antenna system is working in a newly created environment.

PEC
patch

Lumped
port

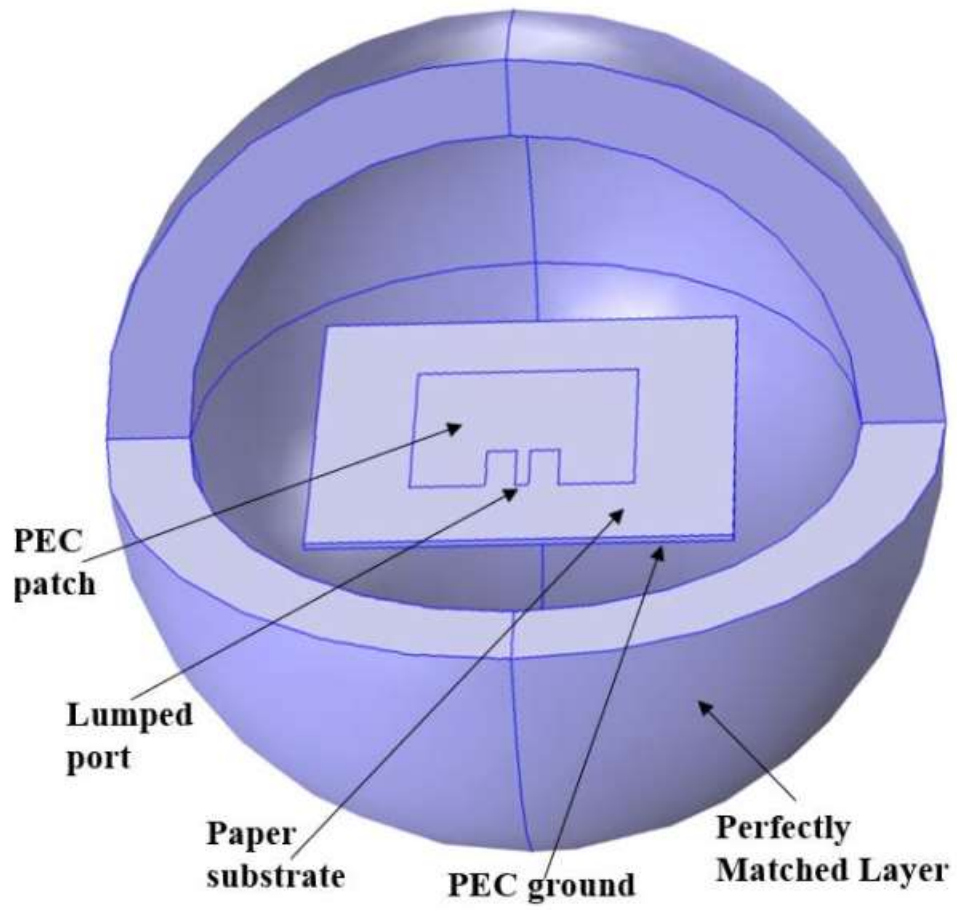Paper
substrate

PEC ground

Perfectly
Matched Layer

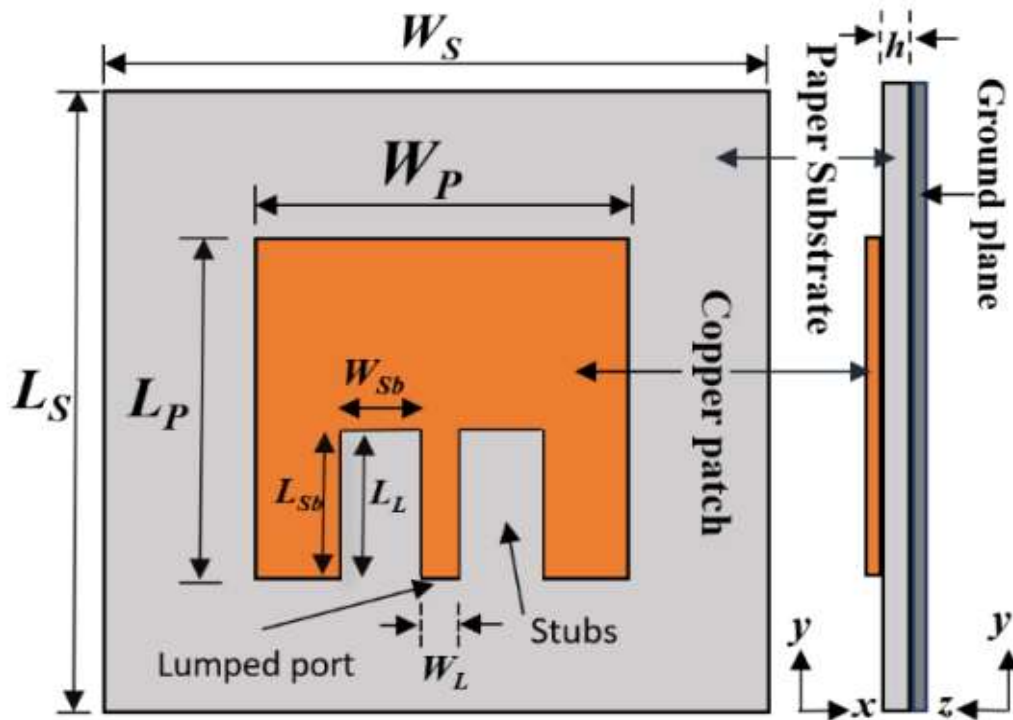Figure 2.1: Design of The Antenna Used [11].

Figure 2.2: Top View and Side View of The Antenna [11].

This figure clearly shows the three different layers of our designed patched antenna where right side shows the side view and the left side shows the top view. In the side view, the right most part is known as the ground plane, the middle portion is known as the substrate and for our purpose paper is used as substrate. In-stead of paper, plastic could have also been used but plastic is not biodegradable and is also costly compared to paper. So, keeping in mind the cost as well as the environment friendliness, paper was selected. The left plane is the patch which is made of copper. A lumped port has also been used in order to excite the designed antenna. The value of the parameters selected for each of the component are given in the table alongside their usual representation.

Table 2.1: Value of different parameters of the antenna.

Parameters	Value	Description
H	1.8 Mm	Thickness of the substrate
Ws	135 Mm	Width of the substrate
Ls	135 Mm	Length of the substrate
Wp	97 Mm	Width of the patch
Lp	95 Mm	Length of the patch
Wsb	9 Mm	Width of the stub
Lsb	19 Mm	Length of the stub
Wl	5.6 Mm	Width of the feedline

.

Chapter 3

Methodology

3.1 Introduction

This study uses two different methods in order to find out which method gives the less error. The methods are:

- ✱ Number 1: Error from S11 calculation.

- ✱ Number 2: Error from FFT calculation.

In the first method mentioned, S11 or in other terms known as the reflection co-efficient is calculated with the help of Comsol Multiphysics which contributes in the simulation part. The most important part is to calculate the lowest values of the reflection parameter as it signifies for the best performance. The study also uses another method, known as the FFT calculation method or the fast Fourier transform method. An algorithm based on the Fourier transform is used in order to find the results in the frequency domain so that the corresponding error can be calculated from there.

3.2 Equations used

In order to find out the results of the simulations performed, different concentration must have some different values based on which the simulations could be run. Here, the changing parameters are Electrical conductivity and Relative permittivity. As we have used paper-based substrate any value between 1-2 can be taken as the Relative permittivity. For our purpose, 1.78 is taken and all the simulations have been run by fixing this value. If the concentration is between 1-5 mol/L then,

$$\epsilon_s = \epsilon_s(w)\ (0.999 + 8.521 \times 10^{-4}tc + 0.0130 - 0.175c + 2.344 \times 10^{-4}t - 1.235 \times 10^{-5}t^2) \qquad (1)$$

$$\varsigma = 0.096tc - 0.8c^2 + 6.554c \qquad\qquad (2)$$

where, ϵ_s is denoted as the Relative permittivity and ς is the electrical conductivity.

But, if the concentration is less than 1 mol/L, then

$$\epsilon_s = \epsilon_s(w)\ (1 - 3.742 \times 10^{-4}tc + 0.034c^2 - 0.178c + 1.515 \times 10^{-4}t - 4.929 \times 10^{-6}t^2) \qquad (3)$$

$$\varsigma = 0.174\ tc - 1.582c^2 + 5.923c \qquad\qquad (4)$$

Here, the t and c represent the temperature and the concentration themselves. The equations will hold for any temperature ranging from 5-35 degree Celcius and for our case the temperature is taken at 20 degree Celcius. The other unknown parameter is the concentration one depends upon the users input like for our case we have performed simulation for different concentrations like 0.3 mol/L or 0.1 mol/L etc.

3.3 Data acquisition and performance

3.3.1 1ˢᵗ Method

In the first method, the error is calculated by finding out the Concentration model for all the different concentrations that we've taken for our purpose. Here, the concentration that we have taken are 0.03 mol/L, 0.05 mol/L, 0.07mol/L , 0.09 mol/L, 0.1 mol/L, 0.2 mol/L. The S11 values are taken from all the different concentrations. S11 values shows the Reflection Co-efficient of a circuit. It normally means how much input power returns back to the source compared to how much goes to the load. Ideally, no power should be coming back to the source. So, the reflection co-efficient should be ideally zero. But for most of the circuits, it doesn't become zero rather it has some value. So, for this study we have taken the minimum value possible for our reflection parameter so that the circuit works at the best condition possible. For all the different concentrations parameter we have plotted the Frequency vs S11 curve in order to find out the lowest possible value of S11 for all the corresponding concentrations. After finding out the lowest

S11 value, corresponding resonant frequency of that reflection co-efficient was found out. Then, plotting is done of the resonant frequency vs concentration from there. Our main goal here is to find out the error that this method gives us. So, after finding out all the points necessary for all the different curves, we have taken an unknown concentration of 0.12 mol/L in order to find out that how much error this actually gives us from the method we have used. In order to find this, we have implemented a mathematical equation which we have made form the six different concentration points that we have used. For this, order ranging from one up to six has been taken as we can have a maximum of seven unknown points from here. For different orders, it will give us different result. We have performed the analysis the same way we have done for the other concentrations for this unknown concentration of 0.12 mol/L. This is the desired value for this concentration. Then, after applying the mathematical formula we can get the actual value for different orders. We can then check the deviation from the original one in order to find out the error. The error or the deviation will basically show us how good our prediction is. This is for the 1st method. Then, we have taken three more concentrations in between the concentrations we have taken already in order to see how linear original curve behaves with the new points.

3.3.2 2nd Method

The 2nd method we have used is for FFT calculation. FFT or more commonly knowns as Fast Fourier Transform is an algorithm which was developed to perform the Fourier transform more efficiently.

We have implemented the Fourier transform to the data that we have collected form the different concentration of all the different plots we have generated. The Fourier transform will give us the result in terms of frequency vs amplitude. After getting the result, we have polished the curve a bit in order to make it a bit smoother so that every point is clearly visible. Furthermore, we have taken five vertical lines at different points which are 50 db,100 db ,150 db, 200 db and 250 db. If we have gone beyond that we then would have gone past the lowest point available for all the different curves. For our purpose we have selected these five lines, however it can be six-seven lines. Moreover, we have taken the points where the vertical lines intersect with the concentration lines.

The points are taken as such. Then the curves are plotted in such a manner to see the concentration vs frequency values from the horizontal lines. It shows us the way the curve moves from the lowest concentration to the upper concentration. These lines show the linear characteristics of the curves plotted. After that the same 0.12 mol/L concentration was plotted by following the same FFT procedure in order to find out the actual result for this value and after that the mathematical equation just like the previous method was formed for all the different orders ranging from 1st order to 6th order but in these case as we have five different lines, we have got six different orders for all these five lines, totaling thirty, unlike the previous method which had only five. After that, the deviation from the original value shows us the amount of error what each line gives and then we can take the lowest amount of error for maximum accuracy.

3.4 Feature Extraction

All the designs were made by using the Comsol Mutiphysics software and all the processing were done in the Matlab environment (For example, Mathworks). Multiple parameters were extracted depending on the methods used from multiple Softwares. A description of the parameters is given below:

(i) S11: Otherwise known as the reflection co-efficient. It is extracted from the Comsol Mutiphysics Software after simulating the different concentration plots.

(ii) FFT: the magnitude and the frequency were calculated after applying the algorithm to the dataset acquired from the simulations performed.

(iii) Error: For the two different methods mathematical equations were created to find the deviance from the original value otherwise known as the error.

(iv) Polyfit: Function used to find out the constant values of the mathematical equations necessary to find out the error.

3.5 Conclusion

After the extraction of the required parameters, the values were set into the different methods used in order to find out the percentage of error in different orders. There may be irregularity in different modes and by performing each and every other modes of operation, we can have a clear picture of how it varies from one order to another.

Chapter 4

Results And Discussion

4.1 Introduction

Data was sorted out by using two different methods where multiple parameters have had significant amount of impact. The parameters were taken care with great precision so that not a single value can be disturbed to get the best possible result available.
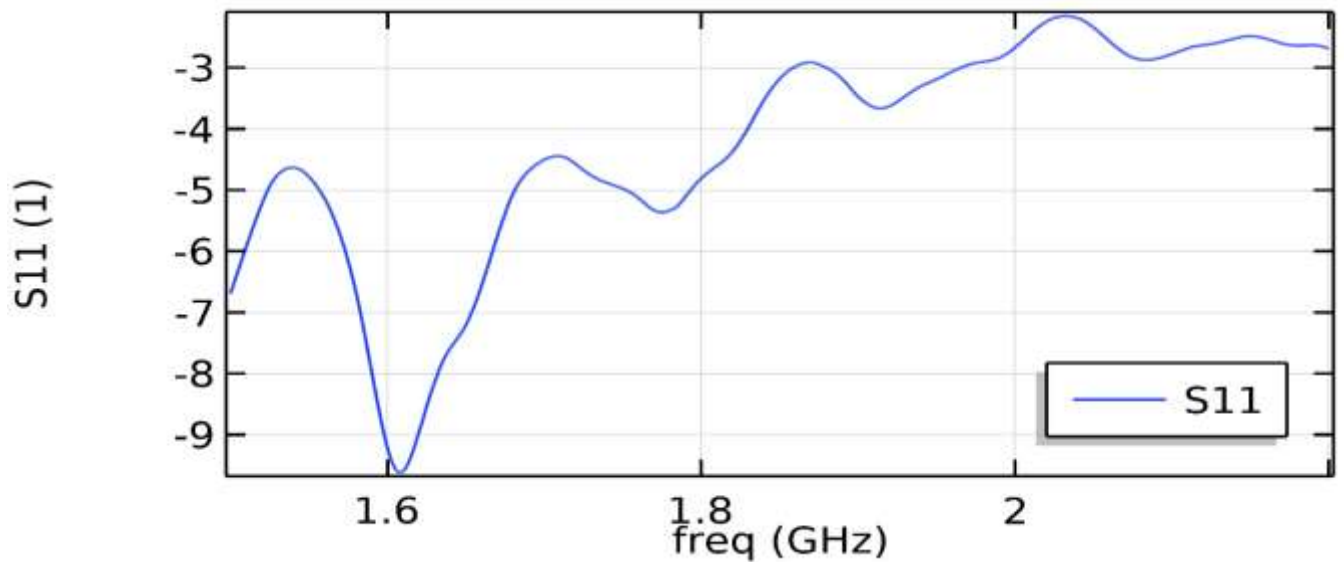
4.2 Result Explanations

Figure 4.1: S11 result for the concentration 0.03 mol/L.

This figure demonstrates the result after simulating the process for the concentration of 0.03 mol/L which gives us the resonant frequency as well as the S11 value, necessary for calculation of the frequency vs Concentration   plot.
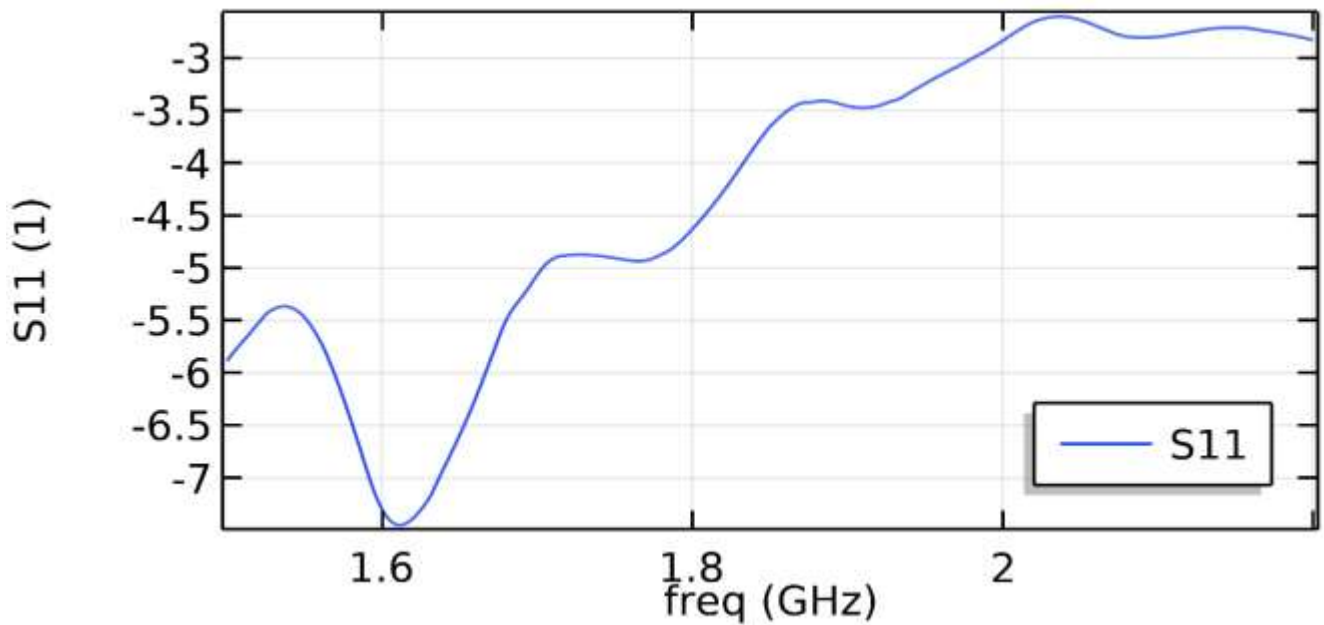

Figure 4.2: S11 result for the concentration 0.05 mol/L.

This figure demonstrates the result after simulating the process for the concentration of 0.05 mol/L which gives us the resonant frequency as well as the S11 value, necessary for calculation of the frequency vs concentration plot.
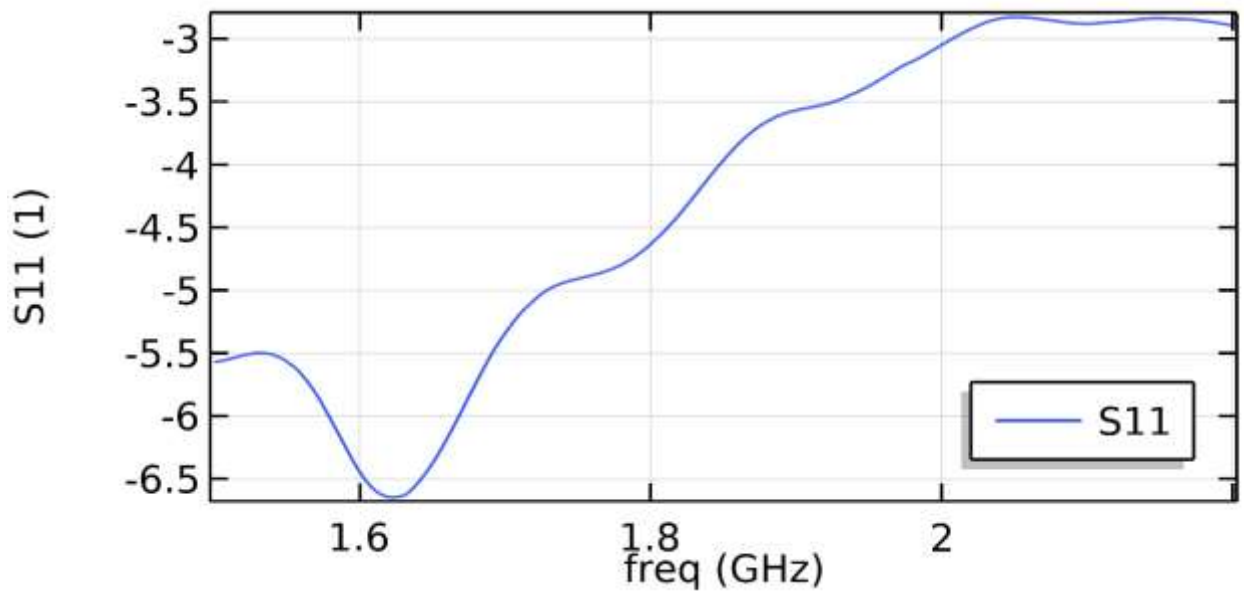
Figure 4.3: S11 result for the concentration 0.07 mol/L.

This figure demonstrates the result after simulating the process for the concentration of 0.07 mol/L which gives us the resonant frequency as well as the S11 value, necessary for calculation of the frequency vs concentration plot.
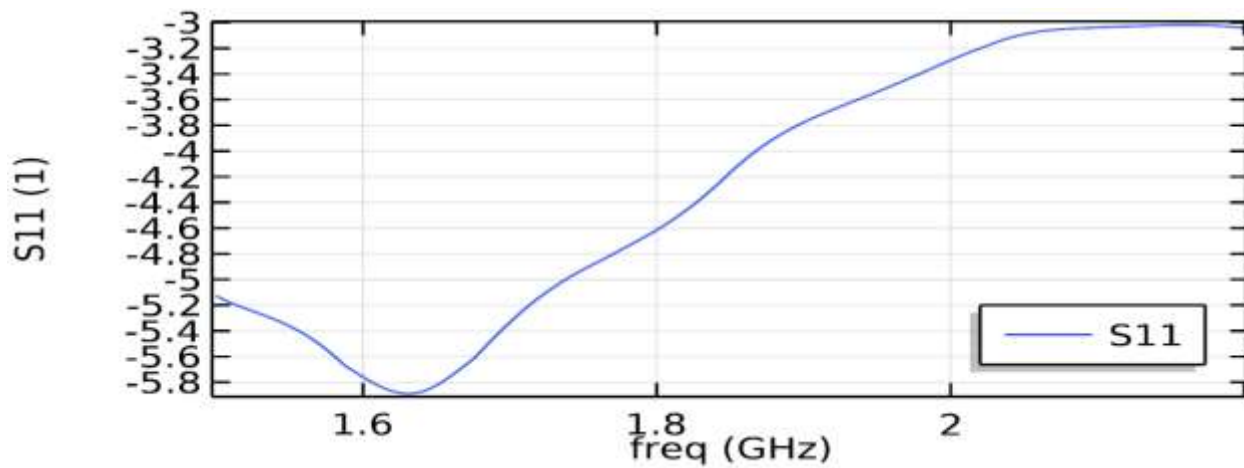

Figure 4.4: S11 result for the concentration 0.09 mol/L.

This figure demonstrates the result after simulating the process for the concentration of 0.09 mol/L which gives us the resonant frequency as well as the S11 value, necessary for calculation of the frequency vs concentration plot.

Figure 4.5: S11 result for the concentration 0.1 mol/L.

This figure demonstrates the result after simulating the process for the concentration of 0.1 mol/L which gives us the resonant frequency as well as the S11 value, necessary for calculation of the frequency vs concentration plot.
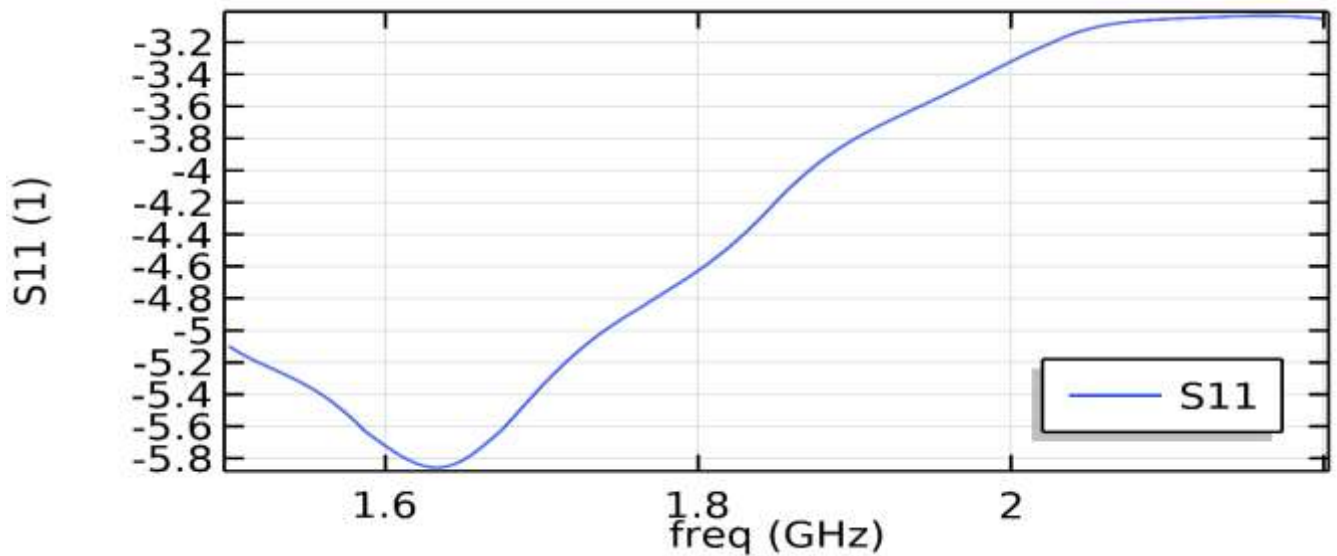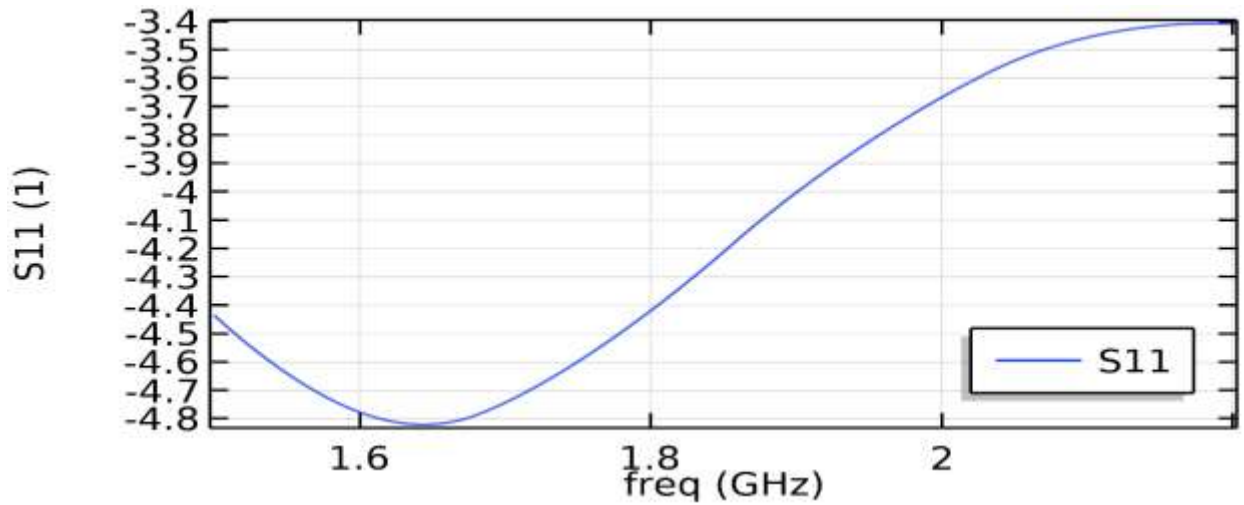
Figure 4.6: S11 result for the concentration 0.2 mol/L.

This figure demonstrates the result after simulating the process for the concentration of 0.2 mol/L which gives us the resonant frequency as well as the S11 value, necessary for calculation of the frequency vs concentration plot.
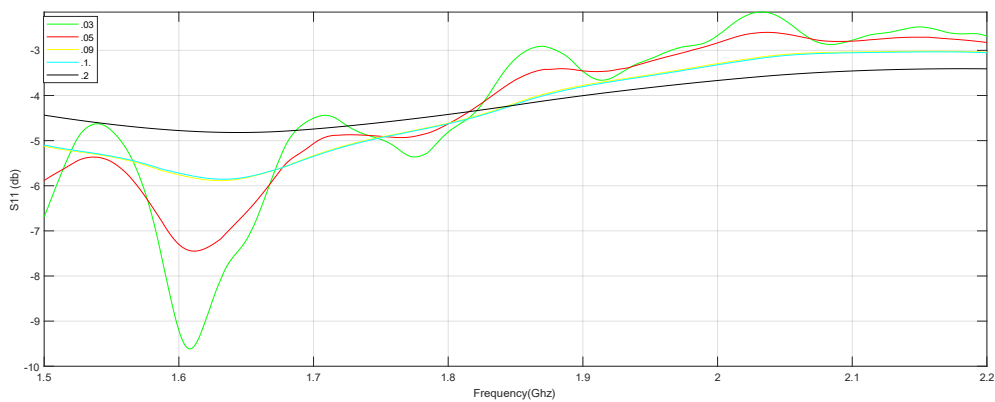

Figure 4.7: S11 value for all concentrations together.

This graph represents all the curves that have been plotted together in a single file in order to easily find out which curve behaves how and what is the real value of the lowest S11 parameter from this graph. The value will help us to further identify the error in order to calculate the deviation from the original value.
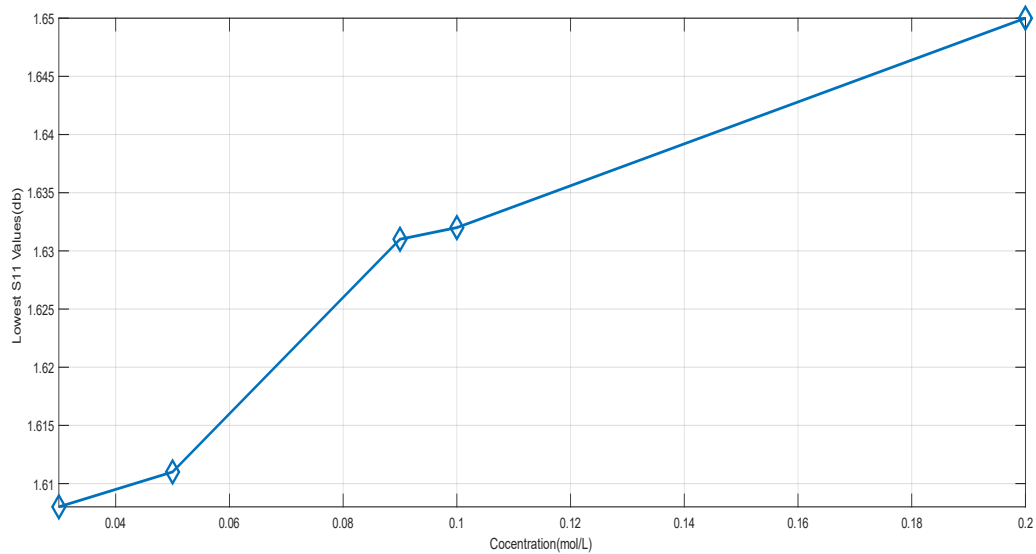

Figure 4.8: Concentration vs S11 value.

This graph represents the Concentration vs the lowest value of S11 taken after performing the simulations for all the concentrations. It shows the value for all the possible lowest S11 value for all the different concentration.
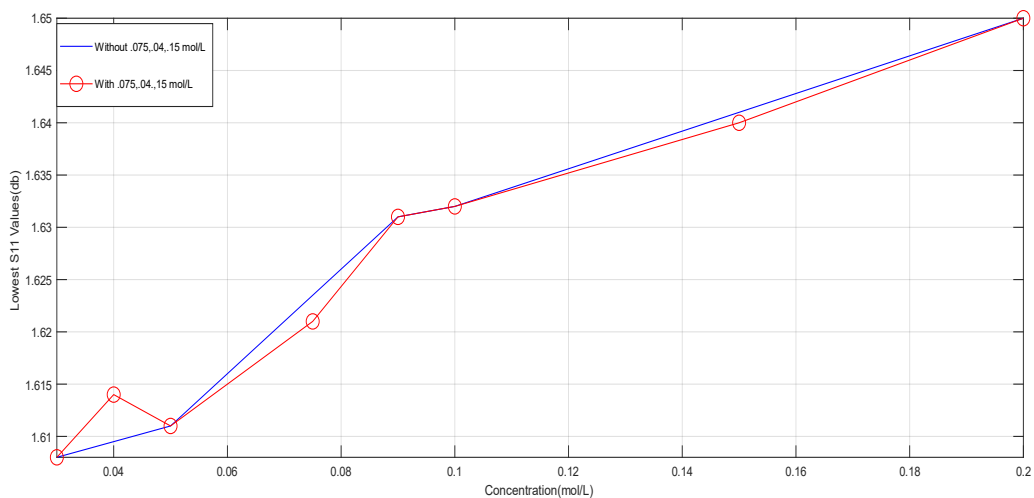
Figure 4.9: Linearity and non-linearity portion.

Three more unknown concentration of 0.075 mol/L, 0.04 mol/L and 0.15 mol/L have been taken in order to see how linearly the curve behaves. It is pretty much prominent from the figure that the curve behaves the best at the right most side, almost linear compared to the previous one but at the left most side it is very non-linear as there is a huge deviation from the original path.
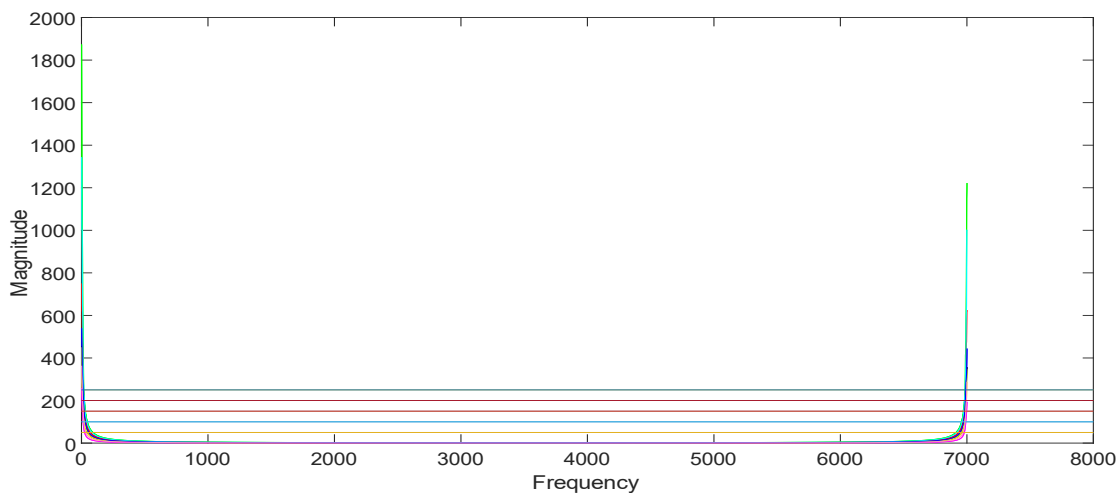
Figure 4.10: Results after applying FFT.

This figure is an actual view figure of the FFT calculation method. Here, after getting the data by performing the simulation, we have performed an algorithm known as the fast Fourier transform. After getting the results, we have taken five different horizontal lines in order to find out the points where they intersect with the curves.
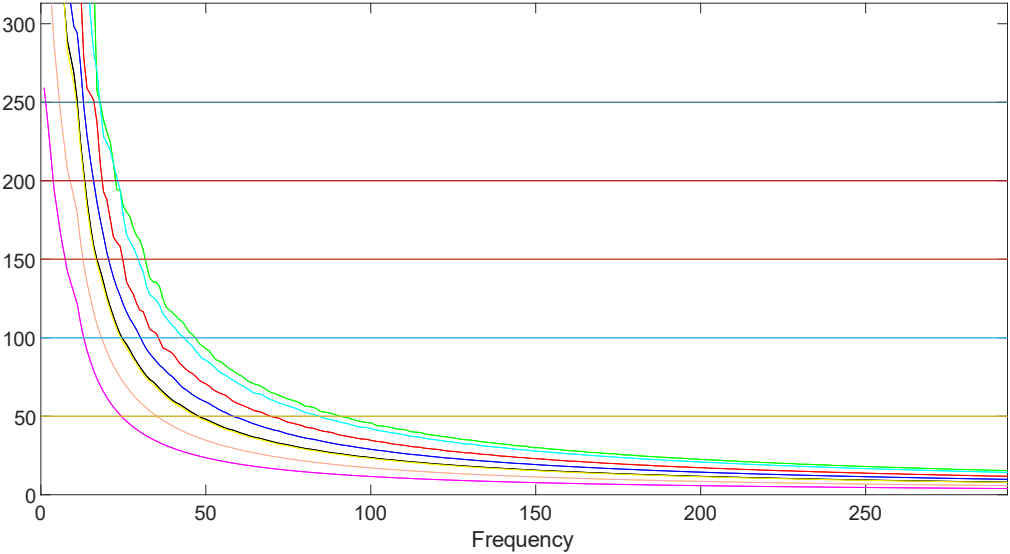
Figure 4.11: Zoomed in version of the FFT plot.

This is a zoomed in version of the figure 4.10.
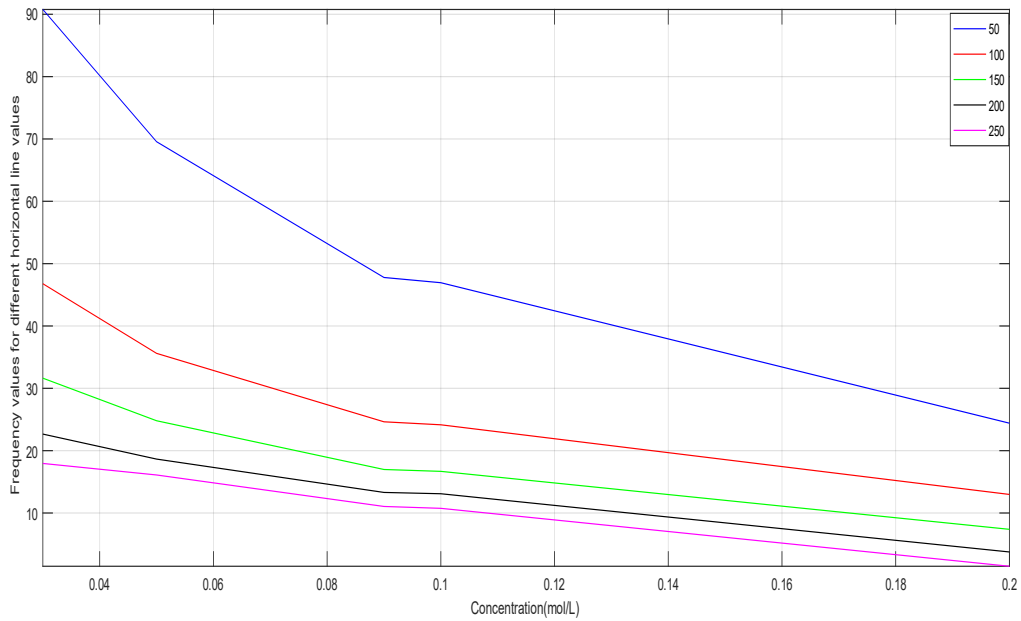
Figure 4.12: Linearity of the horizontal lines.

This plot shows the linearity property of the different horizontal lines taken at five different points as 50 db,100db,150 db,200 db,250 db. It shows the linearity property of the different lines and it is pretty clear that the line 50 db is the most non- linear compared to the other lines and the line 250 db is the most linear compared to the other lines.

Figure 4.13: Percantage of error for the horizontal line 50 db.

This figure demonstrates the percantage of error for the horizontal line 50 db. Different horizontal line will have different amount of error at different orders. It is clear from this figure that which order gives the least amount of error and which order gives the highest amount of error.
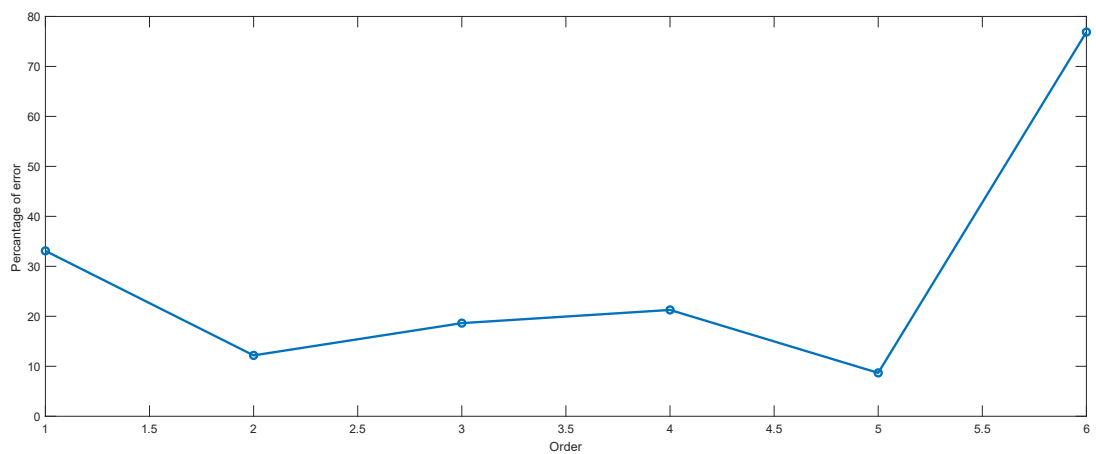
Figure 4.14: Percantage of error For the Horizontal line 100 db.

This figure demonstrates the percantage of error for the horizontal line 100 db. Different horizontal line will have different amount of error at different orders. It is clear from this figure that which order gives the least amount of error and which order gives the highest amount of error.
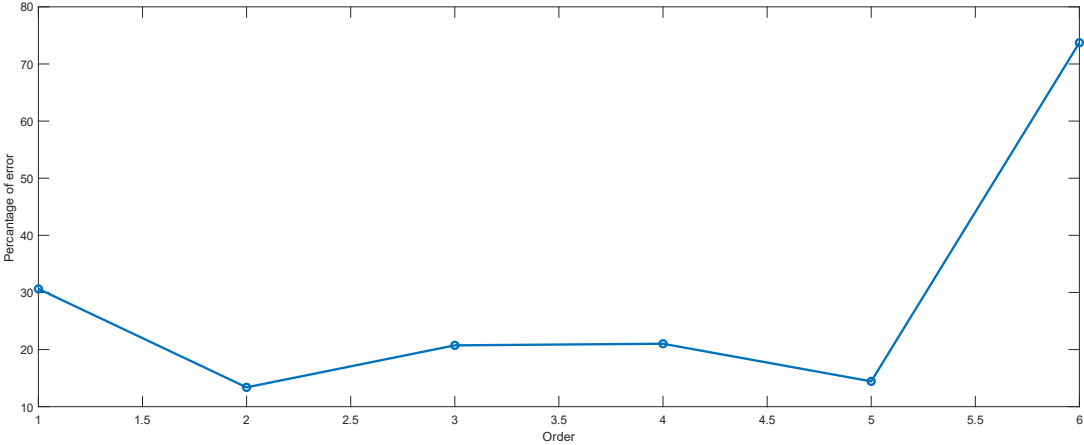
Figure 4.15: Percantage of error for the horizontal line 150 db.

This figure demonstrates the percantage of error for the horizontal line 150 db. Different horizontal line will have different amount of error at different orders. It is clear from this figure that which order gives the least amount of error and which order gives the highest amount of error.
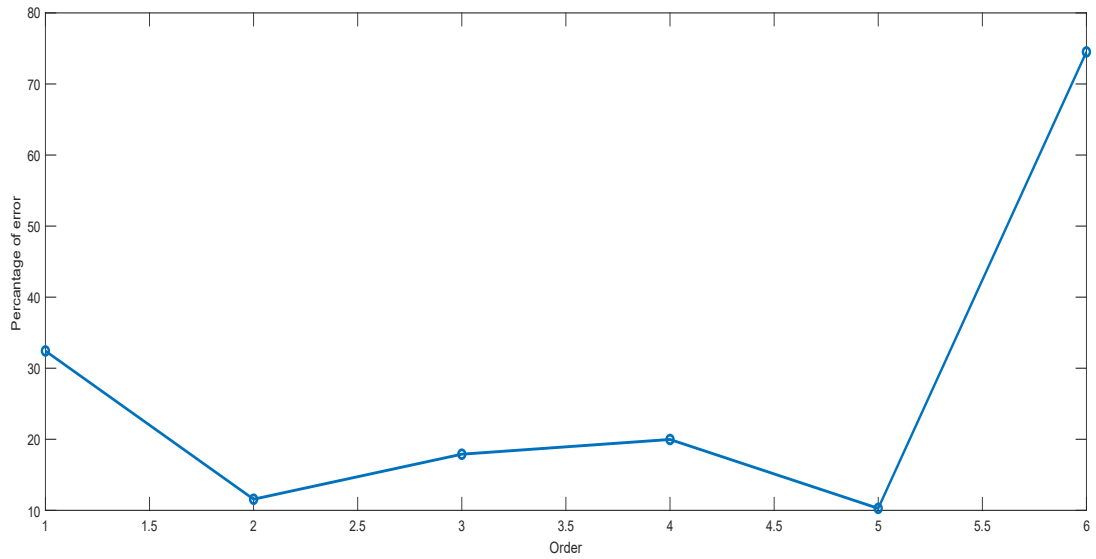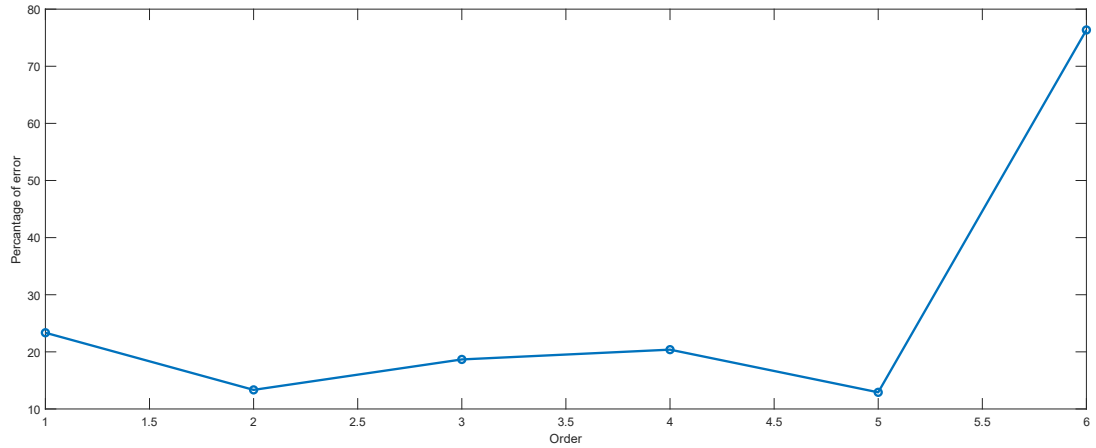
Figure 4.16: Percantage of error for the horizontal line 200 db.

This figure demonstrates the percantage of error for the horizontal line 200 db. Different horizontal line will have different amount of error at different orders. It is clear from this figure that which order gives the least amount of error and which order gives the highest amount of error.
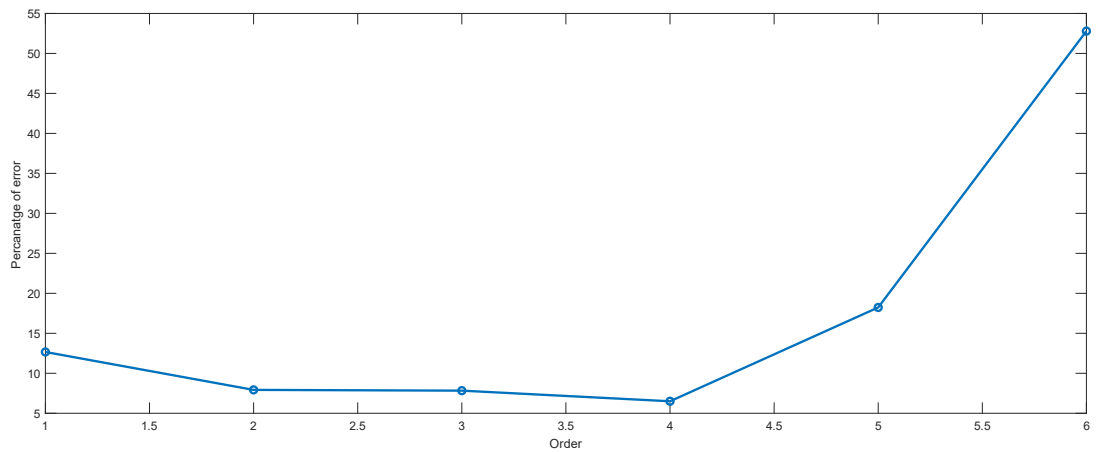
Figure 4.17: Percantage of error for the horizontal line 250 db.

This figure demonstrates the percantage of error for the horizontal line 250 db. Different horizontal line will have different amount of error at different orders. It is clear from this figure that which

order gives the least amount of error and which order gives the highest amount of error.
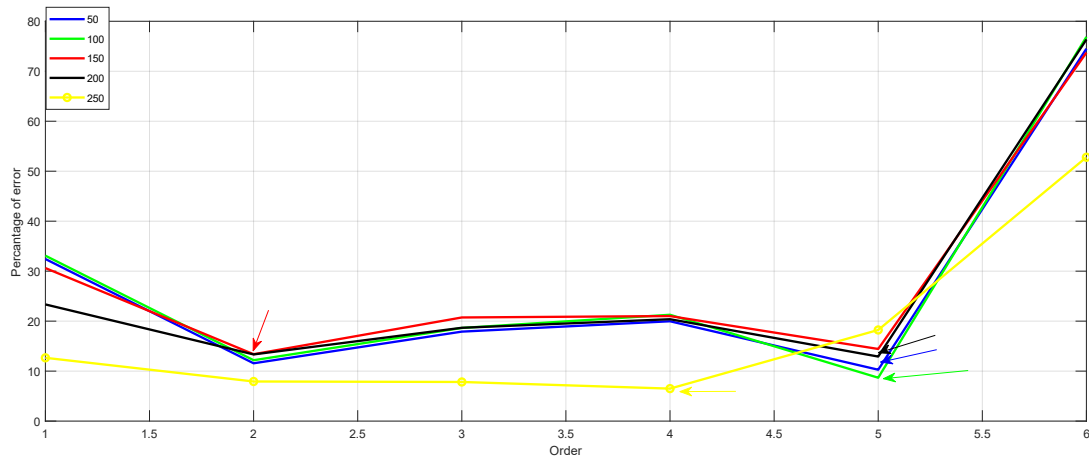

Figure 4.18: Perccantage of error for all the horizontal lines.

For the FFT method, for five different horizontal lines it shows the percentage of error for different orders. For most of the lines, 5th order gives the least amount of error but for some 2nd and 4th can give the least amount of error.
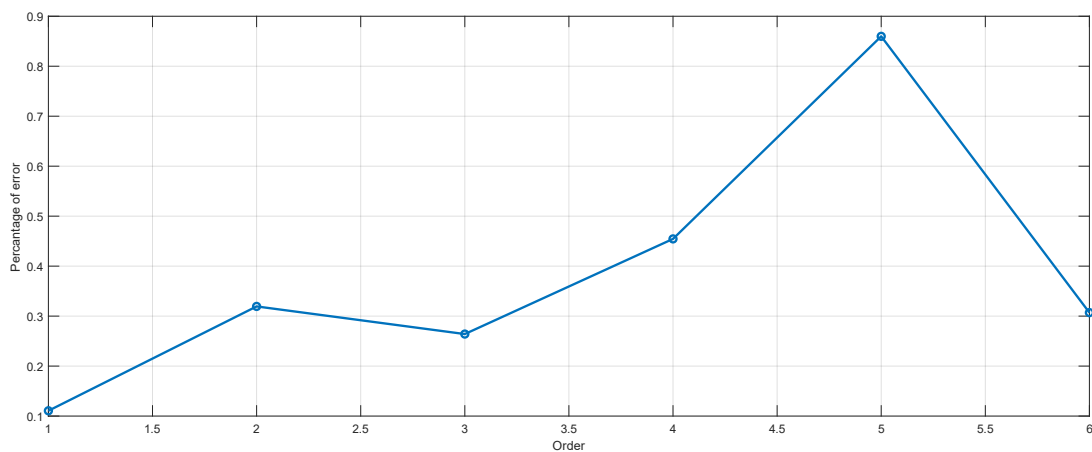
Figure 4.19: Percantage of error from the S11 calculation.

This curve shows the percentage of error for different order for the first method known as the S11 calculation for which 1ˢᵗ order gives the least error unlike FFT method and 5ᵗʰ order gives the highest error.

4.3 Error Calculations

For different orders different percentage of error can be observed. The percentage of error associated with different orders have been shown in the following tables. For each of the methods and horizontal lines, the lowest error is made with bold words to identify easily.

Table 4.1: Error calculation for the S11 method.

Actual Value	Order(N)	Observed value	Error
1.6282	1	1.63	**0.1106**
1.6282	2	1.6334	0.3194
1.6282	3	1.6325	0.2641
1.6282	4	1.6356	0.4545
1.6282	5	1.6422	0.8598
1.6282	6	1.6232	0.307

Table 4.2: Error calculation for the horizontal line 50 db.

Actual Value	Order(N)	Observed value	Error
34.69	1	45.944084	0.324325
34.69	2	38.70248	0.115667
34.69	3	40.9	0.179014
34.69	4	41.61904	0.199742
34.69	5	38..25609	**0.102799**
34.69	6	60.5386	0.745131

Table 4.3: Error calculation for the horizontal line 100 db.

Actual Value	Order(N)	Observed value	Error
17.9	1	23..82446	0.330975
17.9	2	20.08048	0.121815
17.9	3	21.23606	0.186372
17.9	4	21.70831	0.212755
17.9	5	19.45366	**0.086793**
17.9	6	31.7608	0.76876

Table 4.4: Error calculation for the horizontal line 150 db.

Actual Value	Order(N)	Observed value	Error
12.24	1	15.9966	0.306192
12.24	2	13.878	**0.133824**
12.24	3	14.778	0.207353
12.24	4	14.8124	0.210163
12.24	5	13.9942	0.1443317
12.24	6	21.2642	0.737271

Table 4.5: Error calculation for the horizontal line 200 db.

Actual Value	Order(N)	Observed value	Error
9.419	1	11.6182	0.2334486
9.419	2	10.6756	0.133411
9.419	3	11.1776	0.186708
9.419	4	11.3391	0.203854
9.419	5	10.6354	**0.129143**
9.419	6	16.6106	0.763521

Table 4.6: Error calculation for the horizontal line 250 db.

Actual Value	Order(N)	Observed value	Error
7.824	1	8.81288	0.1266391
7.824	2	8.44012	0.079245
7.824	3	8.4365	0.078285
7.824	4	8.3326	**0.065005**
7.824	5	9.2507	0.182349
7.824	6	11.95449	0.527926

4.4 Discussion

The analysis began with S11 calculation method by first getting the lowest S11 value for the resonant frequency at different concentrations. For our purpose, 0.03 mol/L, 0.05 mol/L, 0.07 mol/L, 0.09 mol/L, 0.1 mol/L, 0.2 mol/L concentration have been selected and we performed the analysis for each of them in the Comsol-Mutiphysics Software. After getting the results form there, we have tried to plot the results in a single plot in order to show how every curve behaves and can easily be understood from a single figure.

For our next calculation, we first plotted our desired concentration to their respective lowest value of S11. To find the linearity of curves, three more unknown values are taken in order to find out the linearity of the curves. It is pretty much clear from there that the curve which is actually very close to being linear at the right side where the value of the concentration increases and at the left side it is not close to linear at all.

For the error calculation, From the known values of all other concentrations taken for our analysis, an unknown concentration of 0.12 mol/L is taken in order to find out the percentage of error in this method. A mathematical equation has been created depending on the number of unknowns, in our case ranging from order one to order six and in the unknown constant the value 0.12 mol/L has been set to find out the original values for all the different orders. The deviation from the actual value gives the amount of error and that's how the error at different orders can easily be

understood. The higher the error the higher will be the required storage. So, depending on what people wishes there can be a trade-off between accuracy and cost.

For the second approach, the data that we have collected from the analysis of the curves, an algorithm is further applied there which is known as the Fast Fourier Transform. The "Fast Fourier Transform" (FFT) is an important measurement method in the science of audio and acoustics measurement. It breaks down a signal into its various spectral components and hence offers frequency information. FFTs are employed in machine or system defect analysis, quality control, and condition monitoring. This page describes how an FFT works, as well as the parameters that affect the measurement outcome. The FFT, strictly speaking, is an optimal algorithm for performing the "Discrete Fourier Transformation" (DFT). A signal is sampled over time and its frequency components are separated. Single sinusoidal oscillations at different frequencies, each with its own amplitude and phase, make up these components. After applying the algorithm, we have got the graph which is in the frequency domain and shows the magnitude. Multiple horizontal curves then added with the curves in order to find out the intersecting points which is implemented in order to find the concentration vs the magnitude curve. The curves for the different horizontal lines are plotted in order to show the Linearity behavior. It is pretty much obvious from the curve that the one with the lowest horizontal value shows the minimum linearity and the curve with the highest horizontal value, in this case, which is 250 db shows the maximum linearity. From the different concentration that we have plotted, mathematical equation has been formed. Like the previous case, an unknown, concentration of 0.12 mol/L has also been plotted and FFT algorithm is also applied there in order to find out the original value. After that, in the mathematical equation like the previous one, the unknown values of the constants are formed and the variable value is put 0.12 mol/L in order to find out the error for all the five different horizontal lines from 1st order to 6th order. The values of the percentage of error for all the different lines are then given in the tables and in order to visualize the percentage of error for all the different lines for the two different curves, for both 1st and 2nd method have been generated. However, the result may vary for approaches taken differently and working with different levels of concentration.

Chapter 5

Conclusion

5.1 Introduction

The impact and importance of wearable devices are getting popularity with every passing day. The covid-19 scenario has created a havoc among people and they are now afraid of going to the hospital. In these circumstances, these wearable devices can become the new future and at the same time meet the needs of the people as well. The main thing about these wearable devices is their accuracy. It is related to the health of people. So, these devices must perform well and our target is to provide accuracy of close to 100% every time, otherwise, it won't be as much effective as it is needed to be.

5.2 Future targets

For research in the upcoming future, the things that we have performed for sweat we will try to implement the same things for blood as well as it is very similar in nature and we will compare these two results in order to see if the blood can also be monitored in a similar fashion or other ways are needed to be generated for that purpose. Our main goal for future is to find out the most effective way possible to deliver to the wearable devices so that it can give results that are very accurate. The two methods discussed here have some amount of error, so, we will also try to find out some new methods in order to see how those methods incorporate with the error. Our main goal is to lessen the amount of error by any methods possible. As, in future we are hoping that the demand for these wearable devices will be at it's peak, we will be ready to supply as many of them as needed. The mass production of these devices will not become a problem. Our other goal is to make it's popularity by making another point where people who are afraid of needles can easily

use these devices and need not go to the doctors chamber again. The big data analysis will also be a new addition to these devices. We will try to take the necessary steps in order to find out the weekly health chart of people and at the end of the year, we will provide them with a result that what has happened in the electrolyte level throughout the whole year. This kind of approach will be easier for them to understand and send the report directly to their doctors and take necessary pre-cautions via telemedicine, eliminating the need to ever go to the hospital again. For our research, we will build the physical device and there might be some changes necessary there as the environment will not be ideal like the ones when we have performed the simulations were. So, our first and foremost duty is to make sure that the results do not vary much compared to the obtained results. There may be another problem of taking one single portion of antenna instead of equally sharing the sweat to the whole antenna like in the simulation. So, making sure of that is a pretty daunting task too.

5.3 Conclusion

The two methods discussed here has a promising future and can easily be implemented in the patch antenna design shown. The implementation as well as the building of the physical device may somewhat vary from the results obtained via the software. Some tweaks can easily be made to make sure the physical device also works as accurately as possible to ensure safety and accuracy.

References

[1]A. M. Nia, M. Mozaffari-Kermani, S. Sur-Kolay, A. Raghunathan, and N. K. Jha, "Energy-efficient long-term continuous personal health monitoring," IEEE Trans. Multi-Scale Computing Systems, vol. 1, no. 2, pp. 85–98, 2015.

[2] H. Ghayvat, J. Liu, S. C. Mukhopadhyay, and X. Gui, "Wellness sensor networks: A proposal and implementation for smart home for assisted living," IEEE Sensors Journal, vol. 15, no. 12, pp. 7341–7348, 2015.

[3] S. C. Mukhopadhyay, "Wearable sensors for human activity monitoring: A review," IEEE Sensors Journal, vol. 15, no. 3, pp. 1321–1330, 2015.

[4] O. D. Lara and M. A. Labrador, "A survey on human activity recognition using wearable sensors," IEEE Communications Surveys & Tutorials, vol. 15, no. 3, pp. 1192–1209, 2013.

[5] A. Pantelopoulos and N. G. Bourbakis, "A survey on wearable sensor-based systems for health monitoring and prognosis," IEEE Trans. Systems, Man, and Cybernetics, vol. 40, no. 1, pp. 1–12, 2010.

[6] S. Park, I. Locher, A. Savvides, M. B. Srivastava, A. Chen, R. Muntz, and S. Yuen, "Design of a wearable sensor badge for smart kindergarten," in Proc. IEEE Int. Symp. Wearable Computers, 2002, pp. 231–238.

[7] S. Park, I. Locher, A. Savvides, M. B. Srivastava, A. Chen, R. Muntz, and S. Yuen, "Design of a wearable sensor badge for smart kindergarten," in Proc. IEEE Int. Symp. Wearable Computers, 2002, pp. 231–238.

[8] A. Mosenia, S. Sur-Kolay, A. Raghunathan, and N. K. Jha, "CABA: Continuous authentication based on BioAura," IEEE Trans. Computers, DOI: 10.1109/TC.2016.2622262, 27 Oct., 2016.

[9] A. B. Barreto, S. D. Scargle, and M. Adjouadi, "A practical EMGbased human-computer interface for users with motor disabilities," J. Rehabilitation Research and Development, vol. 37, no. 1, p. 53, 2000.

[10] Arsalan Mosenia, Student Member, IEEE, Susmita Sur-Kolay, Senior Member, IEEE, Anand Raghunathan.Fellow, IEEE, and Niraj K. Jha, Fellow, IEEE, "Wearable Medical Sensor-based System Design: A Survey" DOI 10.1109/TMSCS.2017.2675888, IEEE Transactions on Multi-Scale Computing Systems.

[11] Sakhawat Hossen Rakib, Md. Taslim Reza, Md. Fokhrul Islam, "Design of microstrip patch sensor for non-invasive body electrolyte monitoring", 2020 IEEE Region 10 Symposium (TENSYMP), 5-7 June 2020, Dhaka, Bangladesh.

[12] Razjouyan J, Lee H, Gilligan B, et al. Wellbuilt for wellbeing: Controlling relative humidity in the workplace matters for our health. Indoor Air. 2020;30(1):167-179. doi:10.1111/ina.12618.

[13] Peyman, A., C. Gabriel, and E. H. Grant. "Complex permittivity of sodium chloride solutions at microwave frequencies." Bioelectromagnetics: Journal of the Bioelectromagnetics Society, The Society for Physical Regulation in Biology and Medicine, The European Bioelectromagnetics Association 28, no. 4, pp. 264-274, 2007.

[14] Cuartero, María et al. "Wearable Potentiometric Sensors for Medical Applications." Sensors (Basel, Switzerland) vol. 19,2 363, 2019.

[15] Yeo, J., & Lee, J. I., "Slot-Loaded Microstrip Patch Sensor Antenna for High-Sensitivity Permittivity Characterization." Electronics, vol. 8, no. 5, pp. 502, 2019.

[16] Xu, H., Lu, Y. F., Xiang, J. X., Zhang, M. K., Zhao, Y. J., Xie, Z. Y., & Gu, Z. Z., "A multifunctional wearable sensor based on a graphene/inverse opal cellulose film for simultaneous, in situ monitoring of human motion and sweat." Nanoscale, vol. 10(4), pp. 2090-2098, 2018.

[17] Brendtke R, Wiehl M, Groeber F, Schwarz T, Walles H, Hansmann J, "Feasibility Study on a Microwave-Based Sensor for Measuring Hydration Leve.l Using Human Skin Models." PLoS ONE, 11(4): e0153145, 2016.

[18] Satish, K. Sen and S. Anand, "Design of microstrip sensor for non invasive blood glucose monitoring," 2017 International Conference on Emerging Trends & Innovation in ICT (ICEI), Pune, pp. 5-8, 2017.

[19] Cuartero, María et al. "Wearable Potentiometric Sensors for Medical Applications." Sensors (Basel, Switzerland) vol. 19,2 363, 2019.

[20] C.A. Balanis, Antenna Theory: Analysis and design, 3rd ed., New Jersey: John Wiley &Sons, 2005.